

The Polarity of GaN: a Critical Review

E. S. Hellman¹

¹*Bell Laboratories, Lucent Technologies,*

(Received Tuesday, May 19, 1998; accepted Friday, July 31, 1998)

GaN, AlN and InGaN have a polar wurtzite structure and epitaxial films of these materials typically grow along the polar axis. Although the polarity of these nitrides has been studied by quite a number of techniques, many results in the literature are in conflict. In this paper an attempt is made to lay out a set of polarity assignments to provide a context for discussion of these results. A “standard framework” is proposed to correlate the disparate results, and the framework is used to draw general conclusions about the polarity of bulk crystals, VPE and MBE epitaxial films, and devices.

1 Introduction

Success in the field of nitride semiconductor research has required participants to recognize that the nitrides are very different from the traditional III-V semiconductors. [1]. One important difference that has often been ignored is the fact that epitaxial growth of nitrides is typically done along a polar axis of the material. [a] The polarity has been overlooked for mostly experimental reasons; it has been difficult to measure which polarity is which. For example, convergent beam electron diffraction (CBED) done by different transmission electron microscopists has given contradictory results. Conventional diffraction techniques are prevented by symmetry from distinguishing the two orientations. In addition to the experimental difficulties, discussion of the polarity issue has been hindered by the use of confusing terminology. [2] Recent device work has determined the piezoelectric polarity, but confusion concerning sign conventions for piezoelectric coefficients has left the crystallographic polarity unresolved. This paper will critically review the status of polarity determinations in GaN, including recent work correlating etching, surface structure, and device results. A set of polarity assignments, which we call “the standard framework”, is laid out so that conflicts in the literature can be examined and discussed.

2 Which Face is Which?

Figure 1 illustrates the crystal structure of GaN. Wurtzite GaN, InGaN and AlN epitaxial films are almost always grown with either $[0\ 0\ 0\ 1]$ or $[0\ 0\ 0\ \bar{1}]$ normal to the surface of the film. This orientation occurs on many substrates, even when the substrate is amorphous. The

$[0\ 0\ 0\ 1]$ orientation is known as Ga-face, while the $[0\ 0\ 0\ \bar{1}]$ orientation is known as N-face. Note that polarity is a bulk property, not a surface property. One can imagine a situation where the nitrogen face of GaN would be covered with a monolayer of gallium, but the orientation of the crystal is unchanged. In this paper, we will eschew the use of the term “termination” in favor of the terms “capping” and “polarity”. [2]. “Termination” is the term most often used in the literature on zincblende surfaces to indicate the top layer or capping, but is frequently used in the GaN literature to indicate polarity.

The following sections review the techniques that have been used to study polarity in GaN. A few results from our lab are also presented.

2.1 XPS and Auger studies

The earliest attempt to study the polarity of GaN was reported by Sasaki and Matsuoka. [3] They used MOVPE to grow GaN on both faces of 6H-SiC. Films grown on the C-face had a characteristic rough morphology with large hexagonal crystallites, while films grown on the Si-face had a smooth, featureless morphology. They used X-ray photoemission spectroscopy (XPS) to probe the surfaces of films grown on two faces of SiC. After studying energy shifts of the Ga core-levels, they proposed that the film grown on the C-face was more easily oxidized, and thus likely to be Ga-face. They concluded that Ga-face GaN grows on C-face SiC and that N-face GaN grows on Si-face SiC. The C-face SiC produced films with morphology and photoluminescence similar to that obtained on $(0\ 0\ 0\ 1)$ sapphire under the same conditions. Note that the measurements of Sasaki et al. are not polarity measurements, but rather surface

chemistry measurements, and therefore their polarity determinations should be given less weight than more direct measurements.

Khan et al. [4] attempted to use Auger electron spectroscopy (AES) techniques to determine the polarity of GaN films grown by MOCVD with an AlN buffer layer. This technique measures the composition of the top $\sim 10\text{\AA}$ of the film weighted by the escape probabilities of the Auger electrons. Their calculations indicated that N and Ga “terminated” surfaces should have N/Ga peak ratios of 0.82 and 1.14, respectively. Based on their measured N/Ga ratio of 1.05, they concluded that their films were N-“terminated”. As discussed in the introduction, “termination” is not the same as polarity. An Auger measurement will indeed be sensitive to the capping, but insensitive to the polarity. Note that since this experiment measured only surface properties, there was no particularly good justification for the assignment Ga rich face \leftrightarrow Ga-face (0 0 0 1).

A similar experiment to that of Khan et al. was done in the author’s laboratory. [5] GaN films were grown by molecular beam epitaxy (MBE) on 2 faces ($[0\ 0\ \pm 1]$) of LiGaO_2 . The crystal structure of this material is an oxide with a cation superlattice in the wurtzite structure, resulting in an orthorhombic space group. Epitaxy of GaN on LiGaO_2 has been studied because of its good lattice match to GaN. [6] [7] [8] [9] The $\langle 0\ 0\ 1 \rangle$ direction in LiGaO_2 corresponds to the $\langle 0\ 0\ 0\ 1 \rangle$ direction in GaN. The piezoelectric effect (See Appendix 1) was used to determine the LiGaO_2 polarity. The substrate was broken in two, and GaN films were grown by plasma-MBE with no buffer layer on both sides of the LiGaO_2 simultaneously. A 2x reconstruction was observed on GaN grown on the (0 0 1) (Li,Ga-face) of LiGaO_2 ; no reconstruction was observed on the other face. Figure 2 shows Auger spectra for the N_{KLL} and Ga_{LMM} peaks from the GaN grown on the (0 0 1) (Ga,Li-face) and on the O-face of LiGaO_2 . The N/Ga peak ratio for the GaN grown on the Li,Ga-face was 2.47 ± 0.05 , while that on the O-face was between 2.17 ± 0.05 . Based on the electrostatics of the interfaces, one would expect that N-face GaN should grow on O face LiGaO_2 . In a second growth run using identical growth conditions we grew GaN on ScMgAlO_4 and sapphire. The N/Ga Auger peak ratio was 2.08 for the film on sapphire and 1.94 for the film on ScMgAlO_4 . These films displayed the 3x reconstruction we commonly observed for films grown without AlN buffer layers. According to Khan’s method, the similarity of Auger peak ratios to those measured on films grown on Li,Ga-face LiGaO_2 would indicate that these films are Ga-face, but the RHEED patterns suggest that the surface structure may be different. Given the

large variations from run to run, it seems that surface stoichiometry may be an unreliable indicator of film polarity.

A much more sophisticated technique was employed by Seelmann-Eggebert and co-workers [10] to study the polarity of smooth MOCVD grown films and the two faces of a bulk crystal obtained from crystal growers at UNIPRESS in Poland. They used a technique called hemispherically scanned x-ray photoelectron diffraction (HSXPD), in which the diffraction of a photoemitted electron from surrounding atoms is analyzed. The technique is somewhat surface sensitive, but since it measures relative atom positions, it is a much more direct polarity determination than the techniques discussed above. Bulk crystals of GaN with the platelet growth habit have large (0001) facets. As grown, one side is very smooth, the other side is rough. [11] On annealing at $600^\circ\text{--}900^\circ$ in $\text{H}_2 + \text{NH}_3$, the rough side becomes smooth and the smooth side becomes rough. [11] The HSXPD results strongly indicate that the initially smooth side of the GaN crystal is N-face and the rough side is Ga-face. The smooth MOCVD samples analyzed in Ref. [11] were found to be Ga-face.

We will designate the bulk crystal assignment in reference [10] as the first item in the “standard framework” presented in Section 3.

2.2 TEM Evidence

The first polarity determination for a nitride semiconductor using transmission electron microscopy was done by Ponce et al. [12], for epitaxial films grown by MOCVD on Si-face SiC. They examined lattice images of the interface and studied the bond-length distributions in the interface layer. They differed with the work of Sasaki et al. [3] by concluding that the configuration of the interface was Al-face AlN on Si-face SiC. A subsequent *ab initio* study of AlN on SiC [13] supported Ponce’s assignment.

For reasons that will become clear below, the “standard framework” (Section 3) follows Ponce’s assignment for polarity of GaN on SiC. Thus Sasaki’s assignment is “anti-standard”.

The first attempts by transmission electron microscopists to use convergent beam electron diffraction (CBED) to determine the polarity of GaN single crystals were made by groups at Lawrence Berkeley Lab [14] and Xerox PARC and University of Bristol [15], both in collaboration with the crystal growers at UNIPRESS. In reference [15] by Ponce et al., the smooth face is indicated to be Ga-face (anti-standard), while in reference [14] by Liliental-Weber et al., it is indicated to be N-face, consistent with the determination made by HSXPD [10]. There are no differences in the way these two

groups interpreted their data, so it is not clear why the results from the two groups were different.

Attempts have also been made to use CBED to determine the orientations of epitaxial films. Ponce et al. [15] examined smooth MOCVD films grown on sapphire with a low temperature GaN buffer layer and reported them to be Ga-face [15]. Rouvière et al. [16] studied MOCVD films with various growth conditions. They reported that the smooth films typically obtained with a low temperature buffer layer are predominantly Ga-face, in agreement with Ponce et al., but that films grown directly on sapphire were predominantly N-face. The N-face GaN tends to form hexagonal pyramids with flat tops (or mesas) containing many inversion domains, one of which is situated at the center. Vermaut et al. [17] reported a detailed CBED study of smooth morphology GaN and AlN films grown on Si-face 6H-SiC. They show that the Ga-face GaN and Al-face AlN is obtained on this substrate, in agreement with Ponce et al. [12]

All three of the CBED determinations for GaN films agree that MOCVD GaN films with smooth morphology are Ga-face, strongly suggesting that Sasaki et al. [3] misassigned the Ga and N faces for films on SiC. Based on this agreement, the third element of the “standard framework” (Section 3) is that MOCVD films with hexagonal pyramidal morphology are N-face, while most of the films with smooth morphology are Ga-face.

It should be noted here that while an absolute determination of polarity can be tricky using TEM techniques, relative orientations, and thus inversion domains, can be determined reliably. Cherns observed filamental inversion domains in high quality MOCVD material and identified the nature of the domain boundaries. [18] [19] Romano et al. [20] studied inversion domains in films grown by a variety of techniques and found that their density depended on the growth technique and on the treatment of substrate prior to growth. ECR-MBE films grown on substrates nitrated before growth of the low temperature buffer layer were found to have 50% coverage of inversion domains. Romano and Myers [21] showed that inversion domains can contribute to very rough surface morphology.

2.3 Ion Beam Evidence

Daudin et al. [22] reported a Rutherford backscattering ion channeling technique to study polarity in GaN films. Channels along a $[0\ 1\ \bar{1}\ 2]$ direction are lined by $(0\ \bar{1}\ 1\ 1)$ planes that contain one type of atoms on one side of the channel and the other type of atoms on the other side. Backscattering spectra obtained by tilting the incident ion beam by an angle of $+0.6^\circ$ or -0.6° around this channel are asymmetric, indicating the positions of the Ga and N planes and thus the polarity of the crystal. When applied to single crystals, this technique should

be highly reliable, and the reliability will degrade with the crystallinity of the film. Daudin et al. studied the same films as reference [16] and got consistent polarity determinations, Ga-face for smooth films and N-face for films with hexagonal mesas. A similar study by Crawford [23] found that films grown by ammonia-MBE with AlN buffer layers were also Ga-face.

Time-of-flight scattering and recoil spectroscopy (TOF-SARS) has been used by a group at University of Houston [24] [25] to study the surface composition and structure of GaN films grown by MOCVD. Although this technique is surface sensitive and may depend somewhat on the surface preparation, it measures rather directly the shadowing of gallium atoms by nitrogen atoms, and thus the polarity of the film at the surface. In a film with smooth morphology and nucleated with an AlN buffer layer, the Houston group found strong evidence for a N-face surface [24], contrary to the present paper's “standard framework”. In a second paper [25], they found that the films grown could have either N-face or Ga-face. The N-face surface had much more hydrogen and was much less reactive than the Ga-face. It is not understood what determined the polarity of the two types of films, since the preparation conditions were nominally identical. If these results are correct, then it must be possible to produce by MOCVD films of N-face GaN on sapphire of comparable smoothness to the usual Ga-face films. Another possibility is that the surface preparation for the TOF-SARS, which involves sputtering, modifies the surface polarity or reconstruction.

2.4 Chemical Evidence

It is expected that Ga-face and N-face surfaces of GaN should have quite different chemical properties. Weyher et al. [26] studied the etching of bulk single crystals and MOCVD films in aqueous solutions of KOH and NaOH. They found that the smooth surfaces of GaN bulk crystals etched much more easily than the rough sides. MOCVD films with the two characteristic morphologies (rough with hexagonal crystallites and smooth) were also tested. The rough films with hexagonal crystallites etched much more easily than the smooth films, further linking the smooth film surface with the rough surface of bulk crystals. The ease of etching rough films may be related to the finding of Sasaki et al. [3] that rough films oxidize more easily.

Sun and co-workers [27] studied the thermal stability in hydrogen of GaN films grown by MOCVD on various substrates. They found that films grown on Si-face SiC were stable in hydrogen even at 1000°C , but that films grown on c-plane sapphire (which had the hexagonal pyramid morphology) and a-plane sapphire were strongly attacked. They used the anti-standard polarity

assignment of Sasaki et al. [3] to argue that Ga-face films react more easily with H₂.

Figure 3 shows scanning electron micrographs of 2 GaN films grown by plasma-MBE on (111) silicon substrates in our laboratory. [28] Figure 3a and figure 3b show the as-grown morphology of films grown with (3a) and without (3b) an AlN buffer layer. The film grown with the buffer layer is very smooth, while the film grown without a buffer layer is mostly smooth with hexagonally oriented facets. Figure 4a and figure 4b show the same films after a 10 minute etch in a 1:10 KOH:H₂O solution. The film grown without a buffer layer is etched more rapidly. Figure 5a and figure 5b show the surface morphology obtained by a 45 minute 900°C anneal of the films in a 1:9 H₂:N₂ (forming gas) mixture. Here, the film grown on the AlN buffer layer is more stable, but it accumulates gallium on the surface. The film grown without a buffer layer turns into a spongy mesh, with no gallium accumulation, almost as if the film had a mixture of polarities, and one polarity was completely sublimed. Based on these results, we conclude that whichever assignment is correct, the papers of Sun et al. and Weyher et al. use opposite assignments.

Both these methods are relatively easy ways to investigate the polarity of films. Based on the agreement of HSXPD and 3 groups doing CBED, the “standard framework” posits the less stable surface to be the N-face. This is also consistent with the annealing behavior of the bulk crystals [11]. The N-face may be less stable because nitrogen atoms at the N-face surface can more easily combine in the extremely favorable reactions



A discussion of the relative stabilities of the two surfaces is given by Rapcewicz et al. [29].

2.5 Substrate Studies

Another way to study the properties of films of different polarity is to use polar substrates to produce films of both polarities. We have already discussed experiments comparing films grown on the two faces of LiGaO₂ and the two faces of 6H-SiC. In addition, similar experiments have been done using ZnO and GaAs substrates.

GaN was grown on the 2 faces of ZnO by 2 groups. The author’s group reported [30] that the oxygen incorporation, the carrier concentration, and the Ga droplet formation threshold were different for GaN films grown on the two faces. Our polarity assignment indicated that the oxygen incorporation and resistivity are higher for the GaN grown on the O-face and Ga droplets form more easily on the GaN grown on the Zn-face. Hamdani

et al. [31] found that GaN grown on the oxygen face had more band-edge photoluminescence than films grown on the Zn-face. This could be due to the different oxygen incorporations reported in ref. [30]. It should be noted that polarity assignments in reference [30] are in apparent conflict with other studies of ZnO surface morphology [32]

Growth of both cubic and hexagonal GaN on the Ga- and As- faces of (111)GaAs has been studied by a number of groups [33] [34] [35] [36]. Nagahara et al. [33] found that the GaAs(111)_B surface (As-face) resulted in the highest growth rate by MOVPE. Both Hong et al. [34] and Yang et al. [35] found better quality zincblende GaN on the GaAs(111)_A surface (Ga-face). Cheng et al. [36] found the (111)_B surface to be superior for MBE growth, and in fact they report an inversion of the GaN polarity on (111)_A surfaces, resulting in N-face GaN on both GaAs faces.

Baranowski et al. [37] reported results of MOCVD GaN growth on the two faces of GaN bulk crystals. Growth on the smooth face resulted in a higher threading dislocation density and a large concentration of donors in the film. Growth on the rough face resulted in a much lower dislocation density, but a higher pinhole density.

2.6 Piezoelectric Effects

Perhaps the most direct way to measure the polarity of a GaN film would be to measure the sign of its piezoelectric effect. This is usually quite difficult because of the relatively high conductivity. Recently, however, measurements of heterojunction device structures have rather conclusively determined the dominant piezoelectric polarity in some films. Unfortunately, the piezoelectric polarity and the crystallographic polarity have not been conclusively linked.

Bykhovski and co-workers [38] predicted that the piezoelectric effect at pseudomorphically strained Al_xGa_{1-x}N/GaN heterojunctions can cause a large increase or decrease in the sheet density of the 2-dimension electron gas at a Al_xGa_{1-x}N/GaN interface. Bykhovski and coworkers assumed that the relationship of the piezoelectric axes and the crystallographic axes in GaN had the same sense as found in other III-V semiconductors. (this is opposite to the framework we propose in Section 3). With this assumption, the 2-D electron density *increases* for N-face Al_xGa_{1-x}N-on-GaN interfaces, and for Ga-face GaN-on-Al_xGa_{1-x}N interfaces. The 2D electron gas is *inhibited* for Ga-face Al_xGa_{1-x}N-on-GaN interfaces, and for N-face GaN-on-Al_xGa_{1-x}N interfaces. Asbeck and co-workers [39] obtained similar results, but used opposite assumptions. They showed data indicating that both MBE and

MOCVD grown layers had enhanced electron densities at $\text{Al}_x\text{Ga}_{1-x}\text{N}$ -on-GaN interfaces. Asbeck et al. assumed the *opposite* relationship of the piezoelectric axes and the crystallographic axes (the same one used in our proposed framework). A series of papers by Gaska and coworkers [40] [41] [42] explore some of the device implications of the piezoelectric fields. Their data indicate that MOCVD films can have Ga-polarity, N-polarity, mixed polarity.

Recent calculations of the piezoelectric coefficients referenced to the crystallographic axes by Bernardini, Fiorentini and Vanderbilt [43] have suggested that the sign of the piezoelectric coefficients in AlN, GaN and InN is the same as that found for ZnO and other II-VI materials and *opposite* to those found for other III-V materials. Thus, the experimental results in references [39] [40] [41] [42] which are substantially in agreement, would say that the films are typically Ga-face, as assumed by Asbeck et al., rather than N-face, as assumed by Gaska et al.. This assignment is item 5 in the standard framework. (Section 3)

It should be noted that there are a number of complicating factors for the device measurements. One is the overall strain of the film. It has been shown that the strain which remains in a film after growth can vary from compressive to tensile, depending on the substrate and on the details of the nucleation, growth and annealing conditions. [44] This will add a piezoelectric field normal to the surface which can add or subtract to fields resulting from interface strain. A second complicating factor is the effect of the spontaneous polarization in the wurtzite structure. [43] Unlike the zincblende structure, the wurtzite structure allows the existence of a spontaneous polarization. In a bulk crystal, the spontaneous polarization is typically inaccessible due to screening charges, but in a heterostructure, the difference in the polarization across a heterointerface will result in an interface charge, even in the absence of strain. [45] Finally, non-uniform strains can result in large deviations from the predicted piezoelectric effects.

2.7 Surface Reconstructions as a Probe of Polarity

Two recent publications have established surface reconstructions as a polarity indicator for GaN epitaxial films. In the past, a variety of surface reconstructions have been reported for the polar faces of wurtzite GaN, including (2x2) [46] [47] [48] [49] [50], (4x4) [47], “(3x2)” [50] [51] and (3x3) [52] [53]. Since surface reconstructions are most easily observed by Reflection High Energy Electron Diffraction (RHEED), a technique used routinely in MBE, most reports of surface reconstruction have made on MBE films. Interestingly, many of the early reports were of films not grown directly on

sapphire; the most detailed studies have used MOCVD grown GaN on SiC or sapphire. Reconstructions are sometimes observed during growth depending on the growth conditions. For example, Hacke and coworkers [46] mapped out a (1x1) to (2x2) transition which depended on the Ga/N ratio and temperature during growth. More complex reconstructions, such as (4x4) [47] and (3x3) [53] are typically observed on cooling in Ga rich conditions below 500°C. Most of the reported reconstructions are based only on RHEED, and are thus more accurately described as 2x or 3x patterns. The so-called “(3x2)” pattern, for example, could be a mixture of 2x and 3x patterns, and the (2x2) could be a mixture of (1x2) and (2x1). In our lab, we have made LEED observations of a 6x pattern which was revealed to be a $(3\sqrt{3} \times 3\sqrt{3})R30^\circ$ reconstruction.

In this confusing environment, the recent papers by Smith et al. [54] [55] on STM investigations of GaN surface reconstructions has been an important advance. Smith et al. observe what they believe to be the $(000\bar{1})$ (N-face) surface of a GaN film grown on sapphire by MBE. They observe (1x1), (3x3), (6x6) and $c(6 \times 12)$ surface reconstructions, depending on temperature and Ga coverage. [54] Using MOCVD films as substrates to produce surface they believe to be Ga-face, and observe 2x2, 5x5 6x4 and 1x1 reconstructions at various temperatures. [55] Smith et al. made a polarity assignment based on first-principals calculations of surface superstructures which is consistent with the “standard framework” of the present paper [54], and supported this assignment with etching measurements [55].

The results of Smith et al. have been further tied to polarity assignments for bulk crystals by Held and coworkers [56] who examined films grown on both (0001) and $(000\bar{1})$ faces of bulk GaN. They observe the reconstructions mapped out by Smith et al. on the smooth side of a GaN plate-like bulk crystal, presumed to be N-face, and they find 1x and 2x reconstructions on the “rough” side of the crystal. Thus we can add an item to the “standard framework” for GaN polarity: The clean GaN N-face can be identified by a series of surface reconstructions as described by Smith et al.. The clean Ga-face is characterized by a 2x reconstruction. Some groups report an intense 2x2 during growth of the Ga-face, whereas others can only see this 2x2 during growth interrupts.

Since RHEED patterns with reconstructions have often been reported, the standard polarity assignment can be interlocked with the other standard framework items. Figure 6 shows RHEED patterns observed for the films of figure 3 which were later etched and heated. We find that films which display a strong 3x RHEED pattern are easy-etching, while films which display a strong 2x RHEED pattern are hard-to-etch. Results of Van Hove et

al. [39] [48] [57] and Li et al. [58] link the 2x reconstruction to enhanced 2-d electron gasses at AlGa_xN/GaN interfaces.

It should be cautioned that the effects of hydrogen on surface reconstructions need to be carefully investigated. Calculations by Rapcewicz et al. [29] suggest that hydrogen on either N-face or Ga-face surfaces could result in a 2x2 reconstruction.

3 The Standard Framework

Our discussion above has led us to a set of interlocked characteristics of the two polar (000±1) surfaces of GaN. They are interlocking because if one assignment is wrong, all the others are probably wrong, too. That possibility cannot be categorically ruled out, and as discussed above, there are “anti-standard” results that still deserve serious attention.

The characteristics of the polar faces of GaN are as follows:

1. The smooth side of an un-doped, as-grown GaN plate-like bulk crystal is N-face and the rough side is Ga-face.
2. Ga-face GaN grows on Si-face SiC and N-face GaN grows on C-face SiC.
3. Films with hexagonal pyramidal morphology grown on sapphire are N-face. Smooth films grown by MOCVD are usually Ga-face.
4. The Ga-face of GaN is chemically more stable than the N-face. KOH and NaOH solutions will etch the N-face but not the Ga-face. The N-face will decompose rapidly at 900°C in hydrogen.
5. The relationship of the piezoelectric and crystallographic axes in GaN is like that in ZnO, so that the Ga-face Al_xGa_{1-x}N-on-GaN interface has an enhanced 2-dimensional electron density. (See figure 7(a).)
6. The clean GaN N-face can be identified by a series of surface reconstructions between 100°C and 300°C which include a (3x3) reconstruction. 2x reconstructions are frequently observed on the clean Ga-

With this framework in place, we will now proceed to use the framework to discuss a few polarity-related issues in nitride semiconductor research.

3.1 Polarity and Crystal Growth

It is well known that polarity has strong effects on crystal growth of GaN. The asymmetric habit of bulk crystals is perhaps the plainest indication of this. What has been less clear are the precise processes which manifest the polarity.

GaN is somewhat unusual in that it is typically grown in conditions in which it is not particularly stable. Thus decomposition rates play an unusually important role in processes such as epitaxial growth. [59] Many of the polarity dependent phenomena are thus more easily

explained in terms of the relative decomposition rates than in terms of formation rates. As discussed above, the N-face decomposes more easily than the Ga-face, but this should depend on temperature and the chemical potentials of the constituent atoms (and probably on hydrogen). First-principles calculations of decomposition rates for different surfaces could shed a lot of light on these phenomena.

3.1.1 Bulk Crystals

According to our framework, during growth of GaN bulk crystals from solution, the N-face is in contact with the Ga solution, and the Ga-face is exposed to a nitrogen-rich atmosphere. Based on the various surface stability and annealing measurements that have been done [11] [27], if the situation were reversed, the crystal would decompose.

Recent experiments have shown that the surface morphology of bulk crystals is changed upon doping by magnesium [60].

3.1.2 MOCVD

Smooth epitaxial films grown by MOCVD seem to be mostly Ga-face, although hexagonal pyramidal hillocks are N-face. This could be a simple consequence of the relative stability of polar (1 0 $\bar{1}$ 1) and (1 0 $\bar{1}$ $\bar{1}$) surfaces.

3.1.3 Ammonia MBE

We have observed both 3x and 2x RHEED patterns on GaN grown by ammonia MBE. We observe a large difference (10-20x smaller for 3x) in the growth rate. This is likely to be due to a high decomposition rate for the N-face materials at the high growth temperatures we use.

In general, MBE may be the best technique for producing N-face films. MBE can be done at very low temperatures, and the typical problem is not enough nitrogen rather than too much.

3.1.4 Layer Nucleation

It is typical that growth of GaN on sapphire is successfully accomplished only after painstaking optimization of nucleation conditions, which are the subject of much discussion and lore. This is not so surprising in the context of our polarity discussion, since sapphire is not polar. To grow a unipolar film, tricks must be played to weed out the undesired polarity.

One step that has been observed to have a large effect on film properties on sapphire is the nitridation of the sapphire before growth. [61] De Felice and Northrup [62] have calculated energies for different surface configurations of aluminum nitride bilayers on sapphire. They find that two structures with different AlN polarities are possible, but that only the Al-face structure is stable under typical growth conditions. They argue that the role of the pre-nitridation is to establish the polarity on the surface.

A second step that has been described as “crucial” to the growth of good GaN on sapphire is the high-temperature anneal of a low temperature buffer layer. (An excellent discussion of this process is given in reference [63]). Since the two polarities of GaN are known to have different decomposition rates [11] [27], an important process happening during this step may be the elimination of the N-face nuclei.

3.2 Polarity and Devices

We briefly discuss the implications of the polarity assignment for devices. Figure 7 shows the effect of the strain induced electric field for a heterostructure FET, for a single quantum well, and double heterostructure diode.

3.2.1 FET's

The standard framework implies that normal heterostructure FET's must be grown on Ga-face material. This is fortunate, since one of the most attractive substrates for high-power applications is SiC. The best GaN films on SiC are Ga-face on Si-face, according to our assignment. The inverted structure, with a channel on the growth surface side of a barrier, should work best on N-face material. The only report to date of inverted structure heterostructure GaN FET's [64] has come from an MBE group.

3.2.2 Quantum Wells

Piezoelectric effects in InGaN/GaN quantum wells have recently been a topic of wide interest. Takeuchi et al. [65] discussed how the piezoelectric effect in conjunction with screening causes a blue shift (Stark effect) with excitation in the luminescence from laser structures. They have not discussed what the sign of the piezoelectric effect is, but by analogy to FET's, we can conclude that the piezoelectric effect pushes electrons to the growth-surface side of the well and holes to the substrate-side [66] as shown in figure 7(b), thus reducing the oscillator strength [67] and increasing the laser threshold. It may be that strong piezoelectric fields are what reduces the efficiency of InGaN/GaN quantum wells. Therefore, to make a green or red laser in this material system, it may be necessary to grow on non-polar surfaces or to find a way to apply a compensating bias. In addition, measurements of the bias dependence of the piezoelectric Stark effect should be able to determine film polarity. (This was done by Caridi et al. [68] in the GaAs/AlGaAs system.) Iyechika et al. [66] reported that negative bias on the top electrode resulted in a blue shift of the photoluminescence and used the anti-standard assumption about the piezoelectric coefficients to conclude that their films were nitrogen-face. Chichibu et al [69] have reported that in diode structures, the Stark effect seems not to be very important under typical operating conditions, but that quantum

well photoluminescence was strongly quenched under reverse bias. This suggests that the films are Ga-face and that the junction field is almost perfectly compensating the piezoelectric field in the quantum well.(figure 7(c)) This also suggests that Ga-face n-on-p diodes (such as has been proposed for SiC substrates) won't emit light due to lack of field compensation.

4 Conclusion

Since most polarity determinations for GaN have relied on other polarity determinations in the literature, it has been important to examine both the results and assumptions of previous papers discussing polarity of nitrides. A careful such examination finds that with only a few exceptions, the results which have been reported in the literature are consistent with each other, even though the discussions of these results make conflicting assumptions. It is hoped that the present discussion will facilitate a better understanding of the remaining inconsistencies.

ACKNOWLEDGMENTS

Some of the experiments discussed in this paper were performed in collaboration with D. N. E. Buchanan and E. H. Hartford. The author would like to thank many colleagues for sharing unpublished results, for detailed discussion of published papers, and for many suggestions and corrections to the manuscript.

APPENDICES

1 Sign conventions for the piezoelectric effect.

The piezoelectric constants for AlN, ZnO, and LiGaO₂ have been accurately measured. However, piezoelectric measurements are typically made using a “practical” sign convention, as codified by an IEEE standard [70]. In this convention, the piezoelectric “Z” axis is *defined* such that the piezoelectric coefficient d_{33} is positive. Thus, knowing the measured piezoelectric constants gives us no information about the crystallographic polarity of the crystal unless it is known independently. Bernardini et al. [43] have calculated piezoelectric coefficients referenced to the crystallographic axes, so we can use their calculation to guide us in determining the relation between the practical piezoelectric axes and the crystallographic axes. Their results indicate that the piezoelectric axis Z in GaN is parallel to the crystallographic c-axis, i. e. $\mathbf{z} \parallel [0\ 0\ 1]$. So, if you press on the cation (N, O) face of these crystals with the positive lead of a voltmeter, you will measure a positive voltage transient with a time constant determined by the resistivity and capacitance of the sample. To put it another way, if

you press on the Ga face of an insulating GaN crystal, you induce a polarization that points out of the N face. The electric field in the crystal points from the N face to the Ga-face, so that test electron placed in the crystal will be attracted towards the N-face.

The sense of the piezoelectric axes in AlN, GaN and InN are the same as found for ZnO and other II-VI materials (presumably including LiGaO₂) and opposite to those found for other III-V materials. The sign in GaAs is opposite to that expected for a purely ionic material. In addition to the polarization due to the displacement of ions, there is also polarization of the opposite sign due polarization of the ions themselves. In GaAs, polarization of the ions dominates; in GaN, it is ion displacement that dominates.

REFERENCES

- [a] Zincblende GaN is typically grown along a non-polar axis, in the manner of GaAs growth.
- [1] Shuji Nakamura, Gerhard Fasol, *The Blue Laser Diode - GaN based Light Emitters and Lasers*, (Springer-Verlag, Heidelberg, 1997), .
- [2] See the MIJ-NSR recommendations for polarity nomenclature at <http://nsr.mij.mrs.org/info/diktats.html>
- [3] T. Sasaki, T. Matsuoka, *J. Appl. Phys.* **64**, 4531-4535 (1988).
- [4] M. Asif Khan, J. N. Kuznia, D. T. Olson, R. Kaplan, *J. Appl. Phys.* **73**, 3108-3110 (1993).
- [5] "2-fold and 3-fold Surface reconstructions on (0 0 0 1) GaN", E. S. Hellman, paper N3.38 at the 1996 Fall MRS Meeting, Boston
- [6] P Kung, A Saxler, X Zhang, D Walker, R Lavado, M Razeghi, *Appl. Phys. Lett.* **69**, 2116-2118 (1996).
- [7] J. F. H. Nicholls, H. Gallagher, B. Henderson, C. Trager-Cowan, P. G. Middleton, K. P. O'Donnell, T. S. Cheng, C. T. Foxon, B. H. T. Chai, *Mater. Res. Soc. Symp. Proc.* **395**, 535-539 (1996).
- [8] O. M. Kryliouk, T. W. Dann, T. J. Anderson, H. P. Maruska, L. D. Zhu, J. T. Daly, M. Lin, P. Norris, H. T. Chai, D. W. Kisker, J. H. Li, K. S. Jones, *Mater. Res. Soc. Symp. Proc.* **449**, 123-128 (1997).
- [9] M. A. L. Johnson, S. Fujita, W. H. Rowland, et al, *Sol. St. Electr.* **41**, 213-218 (1997).
- [10] M. Seelmann-Eggebert, J. L. Weyher, H. Obloh, H. Zimmermann, A. Rar, S. Porowski, *Appl. Phys. Lett.* **71**, 2635-2637 (1997).
- [11] G. Nowak, S. Krukowski, I. Grzegory, S. Porowski, J.M. Baranowski, K. Pakula, J. Zak, *MRS Internet J. Nitride Semicond. Res.* **1**, 5 (1996).
- [12] F. A. Ponce, C. G. Van de Walle, J. E. Northrup, *Phys. Rev. B* **53**, 7473-7478 (1996).
- [13] R. Di Felice, J. E. Northrup, J. Neugebauer, *Phys. Rev. B* **54**, R17351 (1996).
- [14] Z. Liliental-Weber, S. Ruvimov, Ch. Kisielowski, Y. Chen, W. Swider, J. Washburn, N. Newman, A. Gassmann, X. Liu, L. Schloss, E. R. Weber, I. Grzegory, M. Bockowski, J. Jun, T. Suski, K. Pakula, J. Baranowski, S. Porowski, H. Amano, I. Akasaki, *Mater. Res. Soc. Symp. Proc.* **395**, 351 (1996).
- [15] F.A. Ponce, D.P. Bour, W.T. Young, M. Saunders, J.W. Steeds, *Appl. Phys. Lett.* **69**, 337-339 (1996).
- [16] J. L. Rouviere, M. Arlery, R. Niebuhr, K. H. Bachem, Olivier Briot, *MRS Internet J. Nitride Semicond. Res.* **1**, 33 (1996).
- [17] P. Vermaut, P. Ruterana, G. Nouet, *Phil. Mag. A* **76**, 1215-1234 (1997).
- [18] D Cherns, WT Young, JW Steeds, FA Ponce, S Nakamura, *Phil. Mag. A* **77**, 273-281 (1998).
- [19] F. A. Ponce, W. T. Young, D. Cherns, J. W. Steeds, S. Nakamura, *Mater. Res. Soc. Symp. Proc.* **449**, 405-410 (1997).
- [20] LT Romano, JE Northrup, MA O'Keefe, *Appl. Phys. Lett.* **69**, 2394-2396 (1996).
- [21] L. T. Romano, T. H. Myers, *Appl. Phys. Lett.* **71**, 3486 (1997).
- [22] B Daudin, JL Rouviere, M Arlery, *Appl. Phys. Lett.* **69**, 2480-2482 (1996).
- [23] Devin Crawford, Ph. D. Dissertation
- [24] M. M. Sung, J. Ahn, V. Bykov, J. W. Rabalais, D. D. Koleske, A. E. Wickenden, *Phys. Rev. B* **54**, 14652-14663 (1996).
- [25] J. Ahn, M. M. Sung, J. W. Rabalais, D. D. Koleske, A. E. Wickenden, *J. Chem. Phys.* **107**, 9577-9584 (1997).
- [26] J. L. Weyher, S. Müller, I. Grzegory, S. Porowski, *J. Cryst. Growth* **182**, 17-22 (1997).
- [27] C. J. Sun, P. Kung, A. Saxler, H. Ohsato, E. Bigan, M. Razeghi, D. K. Gaskill, *J. Appl. Phys.* **76**, 236-241 (1994).
- [28] E. S. Hellman, D. N. E. Buchanan, unpublished.
- [29] K. Rapcewicz, M. B. Nardelli, J. Bernholc, *Phys. Rev. B* **56**, 12725-12728 (1997).
- [30] E. S. Hellman, D. N. E. Buchanan, D. Wiesmann, I. Brener, *MRS Internet J. Nitride Semicond. Res.* **1**, 16 (1996).
- [31] F. Hamdani, A. E. Botchkarev, H. Tang, W. Kim, H. Morkoç, *Appl. Phys. Lett.* **71**, 3111-3113 (1997).
- [32] M. J. Suscavage, D. F. Ryder, P. W. Yip, *Mater. Res. Soc. Symp. Proc.* **449**, 283-288 (1997).
- [33] M Nagahara, S Miyoshi, H Yaguchi, et al., *J. Cryst. Growth* **145**, 197-202 (1994).
- [34] CH Hong, K Wang, D Pavlidis, *J. Electron. Mater.* **24**, 213-218 (1995).
- [35] J. W. Yang, J. N. Kuznia, Q. C. Chen, M. Asif Khan, T. George, M. De Graef, S. Mahajan, *Appl. Phys. Lett.* **67**, 3759-3761 (1995).
- [36] T. S. Cheng, C. T. Foxon, N. J. Jeffs, O. H. Hughes, B. G. Ren, Y. Xin, P. D. Brown, C. J. Humphreys, A. V. Andranov, D. E. Lacklison, J. W. Orton, M. Halliwell, *MRS Internet J. Nitride Semicond. Res.* **1**, 32 (1996).
- [37] J. M. Baranowski, Z. Liliental-Weber, K. Korona, K. Pakula, R. Stepniewski, A. Wyszomolek, I. Grzegory, G. Nowak, S. Porowski, B. Monemar, P. Bergman, *Mater. Res. Soc. Symp. Proc.* **449**, 393-404 (1997).
- [38] Alexei Bykhovski, Boris Gelmont, Michael Shur, *J. Appl. Phys.* **74**, 6734-6739 (1993).
- [39] P.M. Asbeck, E.T. Yu, S.S. Lau, G.J. Sullivan, J. Van Hove, J. Redwing, *Electron. Lett.* **33**, 1230-1231 (1997).
- [40] R Gaska, JW Yang, A Osinsky, AD Bykhovski, MS Shur, *Appl. Phys. Lett.* **71**, 3673 (1997).

- [41] R. Gaska, J. W. Yang, A. D. Bykhovski, M. S. Shur, *Appl. Phys. Lett.* **71**, 3817-3819 (1997).
- [42] R. Gaska, J. W. Yang, A. D. Bykhovski, M. S. Shur, V. V. Kaminskii, S. Soloviov, *Appl. Phys. Lett.* **72**, 64-66 (1998).
- [43] F. Bernardini, V. Fiorentini, D. Vanderbilt, *Phys. Rev. B* **56**, R10024 (1997).
- [44] C. Kisielowski, J. Krüger, S. Ruvimov, T. Suski, J. W. Ager, E. Jones, Z. Lilienthal-Weber, M. Rubin, M. D. Bremser, R. F. Davis, *Phys. Rev. B* **54**, 17745 (1996).
- [45] F. Bernardini, V. Fiorentini, unpublished.
- [46] P. Hacke, G. Feuillet, H. Okumura, S. Yoshida, *Appl. Phys. Lett.* **69**, 2507-2509 (1996).
- [47] K IWATA, H ASAHI, SJ YU, K ASAMI, H FUJITA, M FUSHIDA, S GONDA, *Jpn. J. Appl. Phys.* **35**, L289 (1996).
- [48] J. M. Van Hove, G. Carpenter, E. Nelson, A. Wowchak, P. P. Chow, *J. Cryst. Growth* **164**, 154 (1996).
- [49] W. S. Wong, N. Y. Li, H. K. Dong, F. Deng, S. S. Lau, C. W. Tu, J. Hays, S. Bidnyk, J. J. Song, *J. Cryst. Growth* **164**, 159 (1996).
- [50] M. A. L. Johnson, Shizuo Fujita, W. H. Rowland, K. A. Bowers, W. C. Hughes, Y. W. He, N. A. El-Masry, J. W. Cook, J. F. Schetzina, J. Ren, J. A. Edmond, *J. Vac. Sci. Technol. B* **14**, 2349-2353 (1996).
- [51] W. C. Hughes, W. H. Rowland, M. A. L. Johnson, Shizuo Fujita, J. W. Cook, J. F. Schetzina, J. Ren, J. A. Edmond, *J. Vac. Sci. Technol. B* **13**, 1571-1577 (1995).
- [52] R.J. Molnar, R. Singh, T.D. Moustakas, *J. Electron. Mater.* **24**, 275 (1995).
- [53] E. S. Hellman, C. D. Brandle, L. F. Schneemeyer, D. Wiesmann, I. Brener, T. Siegrist, G. W. Berkstresser, D. N. E. Buchanan, E. H. Hartford, Jr., *MRS Internet J. Nitride Semicond. Res.* **1**, 1 (1996).
- [54] A. R. Smith, R. M. Feenstra, D. W. Greve, J. Neugebauer, J. E. Northrup, *Phys. Rev. Lett.* **79**, 3934 (1997).
- [55] A. R. Smith, R. M. Feenstra, D. W. Greve, M. S. Shin, M. Skowronski, J. Neugebauer, J. E. Northrup, *Appl. Phys. Lett.* **72**, 2114-2116 (1998).
- [56] Ruediger Held, Sean M. Seutter, Brian E. Ishaug, Alexander Parkhomovsky, Amir M. Dabiran, Philip I. Cohen, Grzegorz Nowak, Izabella Grzegory, Sylwester Porowski, unpublished.
- [57] J. Van Hove, private communication
- [58] L. K. Li, J. Alperin, W. I. Wang, D. C. Look, D. C. Reynolds, *J. Vac. Sci. Technol. B* **16**, 1275-1277 (1998).
- [59] N. Newman, J. Ross, M. Rubin, *Appl. Phys. Lett.* **62**, 1242-1244 (1993).
- [60] M. Bockowski, I. Grzegory, S. Krukowski, M. Leszczynski, E. Litwin-Staszewska, B. Lucznik, G. Nowak, T. Suski, H. Teisseyre, J. L. Weyher, M. Wroblewski, S. Porowski, unpublished.
- [61] S. Keller, B. P. Keller, Y.-F. Wu, B. Heying, D. Kapolnek, J. S. Speck, U. K. Mishra, S. P. DenBaars, *Appl. Phys. Lett.* **68**, 1525-1527 (1996).
- [62] R. Di Felice, J. E. Northrup, unpublished.
- [63] X. H. Wu, D. Kapolnek, E. J. Tarsa, B. Heying, S. Keller, B. P. Keller, U. K. Mishra, S. P. DenBaars, J. S. Speck, *Appl. Phys. Lett.* **68**, 1371-1373 (1996).
- [64] O. Aktas, Z.F. Fan, A. Botchkarev, S.N. Mohammad, M. Roth, T. Jenkins, L. Kehias, H. Morkoc, *IEEE Electron Dev. Lett.* **18**, 293-295 (1997).
- [65] T. Takeuchi, S. Sota, M. Katsuragawa, M. Komori, H. Takeuchi, H. Amano, I. Akasaki, *Jpn. J. Appl. Phys.* **36**, L382 (1997).
- [66] Y. Iyechika, Y. Ono, T. Takada, *Mater. Sci. Forum* **264/268**, 1307-1310 (1998).
- [67] J. S. Im, H. Kollmer, J. Off, A. Sohmer, F. Scholz, A. Hangleiter, *Phys. Rev. B* **57**, R9435 (1998).
- [68] E. Caridi, T. Y. Chang, K. W. Goosen, L. F. Eastman, *Appl. Phys. Lett.* **56**, 659 (1990).
- [69] Shigefusa Chichibu, Takayuki Sota, Kazumi Wada, Shuji Nakamura, *J. Vac. Sci. Technol. B* **16**, 2204-2214 (1998).
- [70] T. R. Meeker, *IEEE Trans. Ultrason. Ferr. Freq. Contr.* **43**, 717 (1996).

FIGURES

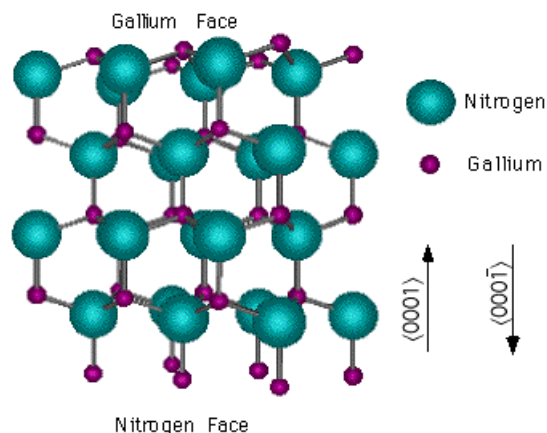


Figure 1. The wurtzite crystal structure of GaN, showing the conventions used to discuss its polarity. The size of the spheres indicates the ionic radius; note that in diagrams which use covalent radii, the gallium's are bigger than the nitrogen's.

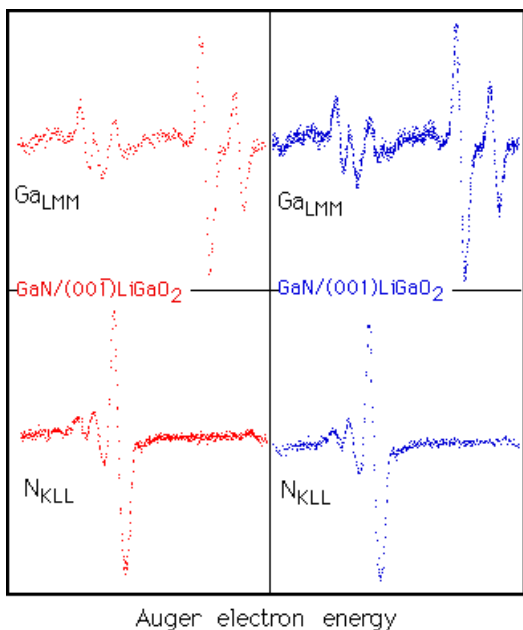


Figure 2. Use of Auger to determine surface composition for GaN films grown on two faces of LiGaO₂. The N/Ga ratio is larger for GaN grown on the O face ((00T)) of LiGaO₂.

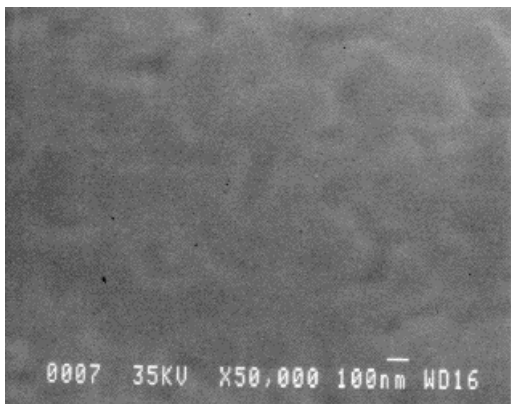


Figure 3a. SEM micrograph of a GaN film grown on an AlN buffer layer on (111) Si. The smooth morphology is characteristic of Ga-face material according to the standard framework.

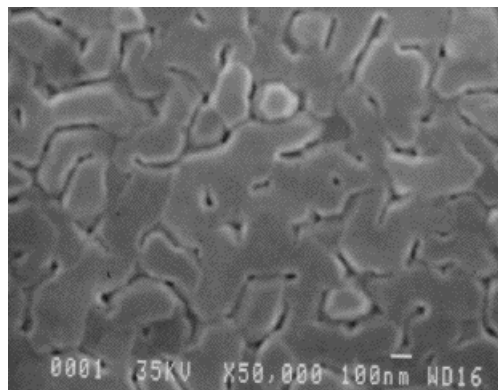


Figure 3b. SEM micrograph of a GaN film nucleated directly on a (111) Si substrate. The flat surfaces and hexagonal faceting are characteristic of N-face material according to the standard framework..

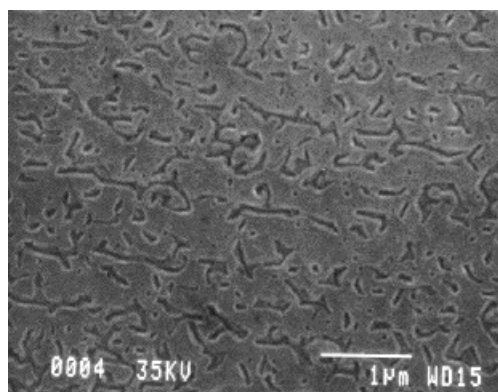


Figure 4a. SEM micrograph of the sample of figure 3a, after etching in 1:10 KOH:H₂O for 10 minutes. The overall etch rate was very small, <10Å/min; the principal effect is the decoration of the microstructure.

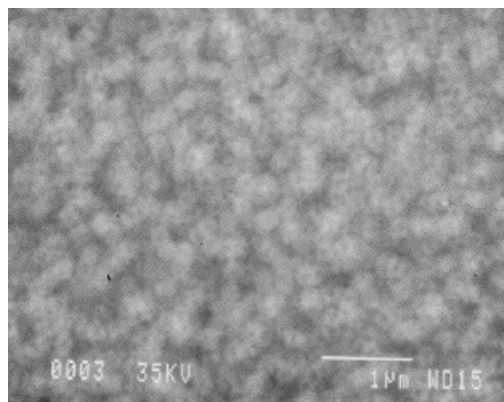


Figure 4b. SEM micrograph of the sample of figure 3b, after etching in 1:10 KOH:H₂O for 10 minutes. The overall etch rate was higher than in figure 4a, about 100Å/min.

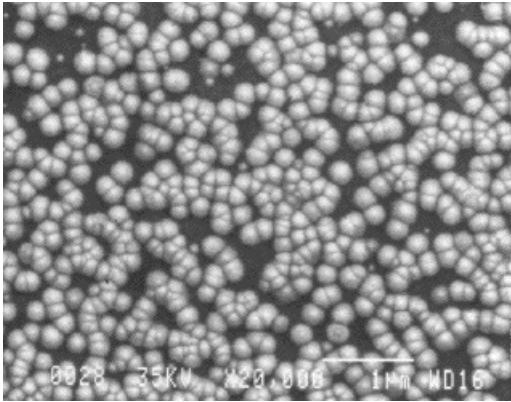


Figure 5a. SEM micrograph of the sample of figure 3a, after annealing in forming gas for 45 minutes at 900°C. The nodules are gallium.

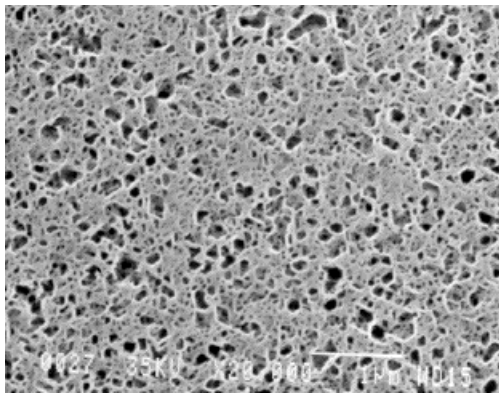


Figure 5b. SEM micrograph of the sample of figure 3b, after annealing in forming gas for 45 minutes at 900°C. Note the spongy network that remains.

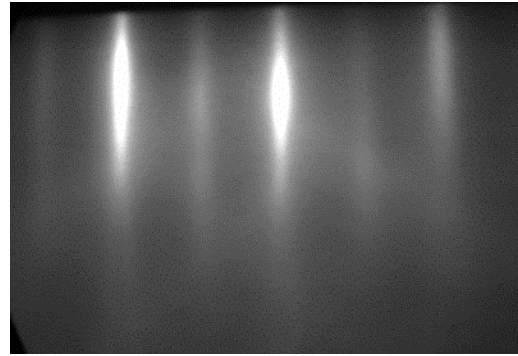


Figure 6a. RHEED pattern from GaN, along the $\langle 11\bar{2}0 \rangle$ azimuth for sample B, showing a strong 2x reconstruction. This reconstruction is associated with Ga-face GaN in the standard framework. This pattern is obtained by cooling the film of Figure 3a to about 400°C after growth. A fraction of a monolayer of Ga is then deposited in vacuum.

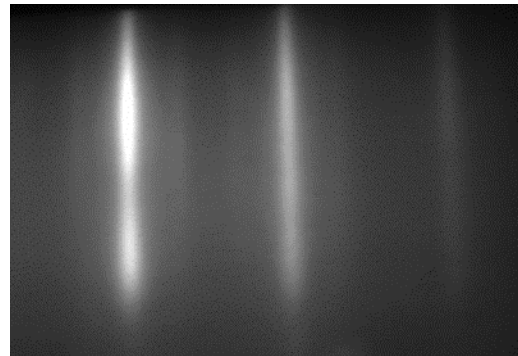


Figure 6b. RHEED pattern from GaN, along the $\langle 11\bar{2}0 \rangle$ azimuth for sample B, showing a weak 3x reconstruction. This reconstruction is associated with N-face GaN in the standard framework. This pattern is obtained by cooling to about 300°C after growth of the film of figure 3b.

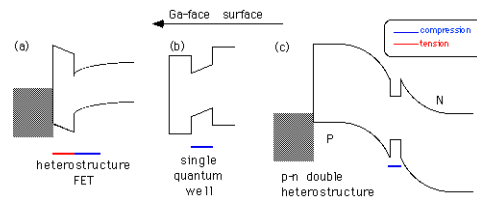


Figure 7. Band diagrams for “standard framework” Ga-face heterostructures.